Carbohydrate Polymer Technologies and Applications 5 (2023) 100310

Contents lists available at ScienceDirect

Carbohydrate Polymer Technologies and Applications

journal homepage: www.sciencedirect.com/journal/carbohydrate-polymer-technologies-and-applications

Kombucha fermentation in yerba mate: Cellulose production, films formulation and its characterisation

Yuly A.Ramírez Tapias [a,b,*], M.Victoria Di Monte [a], Mercedes A. Peltzer [a,b], Andrés G. Salvay [a]

[a] Departamento de Ciencia y Tecnología, Universidad Nacional de Quilmes, Roque Sáenz Peña 352, Bernal, Buenos Aires B1876BXD, Argentina
[b] Consejo Nacional de Investigaciones Científicas y Técnicas (CONICET), Godoy Cruz 2290, Ciudad Autónoma de Buenos Aires (CABA) C1425FQB, Argentina

ARTICLE INFO

Keywords:
Bacterial cellulose
SCOBY
Ilex paraguariensis
Polyphenols
Antioxidant activity
Food packaging

ABSTRACT

The production of Kombucha fermented beverage generates a side-stream composed of bacterial cellulose, a source of biopolymer to develop food contact materials. This work aims to study Kombucha fermentation in yerba mate infusion to maximise cellulose production and its processing for film formulation. Yerba mate infusion with sucrose resulted in an extraordinary substrate for Kombucha fermentation with an optimised cellulose production of 19.4 g/l and 0.29 g/g of yield. Filmogenic dispersions were analysed in terms of rheology and particle size distribution. Microscopic characterisation of films exhibited homogeneous surfaces. The addition of glycerol, as well as the solids from the fermented broth, resulted in a significant increase in hydration and a reduction in elastic modulus, ultimate tensile strength and glass transition temperature of the films. The results revealed that the formulation containing the Kombucha fermented media showed similar properties to the glycerol plasticised material. This could be considered a novel result as it may replace the use of traditional plasticisers. Bioactive compounds from yerba mate provided an antioxidant activity greater than 95% of ABTS radical inhibition to cellulosic material, demonstrating that natural bioactive cellulose-based films are materials that potentially protect food products against oxidation.

Introduction

Kombucha is known worldwide as a probiotic beverage as it contains live microorganisms in its composition (Chakravorty et al., 2019). This beverage is produced through the fermentation of sugared tea with an inoculum of SCOBY (symbiotic community of bacteria and yeast). Traditionally, it is prepared with black tea, which confers healthy properties to consumers due to the main compounds found in this type of tea as alkaloids (caffeine, theobromine, and theophylline) and polyphenols (catechins, theaflavins, and thearubigins) (Chakravorty et al., 2019; Silva Júnior et al., 2021).

During Kombucha fermentation, it is produced as a side-stream, a floating pellicle composed of cellulose that is synthesized by acetic acid bacteria (AAB). The bacterial cellulose (BC) pellicle is formed in the liquid-air interface due to the high demand for oxygen in acetic acid bacteria metabolism, and it acts as a defence against external contamination protecting the equilibrium amongst SCOBY species (May et al., 2019). A fraction of this material can be used as inoculum for subsequent fermentations but it is commonly discarded. However, the BC pellicle has excellent film-forming properties as was demonstrated in previous work (Ramírez Tapias et al., 2020). The bacterial nature of this cellulose by-product provides exceptional properties to the material as high purity (it is free from plant components such as hemicelluloses and lignin), great mechanical strength due to the network of nanofibrils, high degree of polymerization, crystallinity, water holding capacity, chemical stability and biological adaptability (Cottet et al., 2020; Mokhena & John, 2019).

Recently, it has been formulated Kombucha analogues using different vegetable raw materials in the culture broth; such as *Brassica tournefortii* leaves (Rahmani et al., 2019), coffee (Bueno et al., 2021), pitanga, *Eugenia uniflora L.* and umbu-cajá, *Spondia tuberosa* (Silva Júnior et al., 2021), and infusions from yerba mate, lavender, green tea, oregano and fennel (Ramírez Tapias et al., 2022). These new preparations offer variations in flavours, sources of phenolic compounds with antioxidant capacity, and different nutrients. Concerning these changes of substrates for Kombucha preparations, it was also identified differences in cellulosic material yield production. Kombucha cultured in yerba mate infusions demonstrated high cellulose production with

* Corresponding author at: Departamento de Ciencia y Tecnología, Universidad Nacional de Quilmes, R. Sáenz Peña 352, Bernal, Buenos Aires B1876BXD, Argentina.
E-mail addresses: yuly.tapias@unq.edu.ar, yulyramirez@gmail.com (Y.A.Ramírez Tapias).

https://doi.org/10.1016/j.carpta.2023.100310

Available online 9 March 2023

exceptional antioxidant activity in both fractions, the beverage, and the cellulosic by-product (Ramírez Tapias et al., 2022).

Yerba mate (*Ilex paraguariensis* St. Hil) is a perennial shrub (*Aquifoliaceae*) native to the subtropical region of South America, where it is grown and harvested to obtain its leaves for the commercial processing of yerba mate products (Butiuk et al., 2021a). The infusion of yerba mate is the most popular tea-like beverage in southern Latin American countries, mainly in Paraguay, Argentina, Uruguay, and South Brazil. Its health benefits such as stimulating effect and antioxidant activity are attributed predominantly to polyphenolic compounds (chlorogenic acid) and xanthines (caffeine and theobromine). Also alkaloids such as caffeic acid, flavonoids, saponins, minerals (P, Fe, Ca, and Al), and vitamins (C, B1, and B2) (Burris et al., 2012; Butiuk et al., 2021b; Gullón et al., 2018). The synergistic of these compounds and Kombucha SCOBY dynamics produced a high microbial population and an important amount of cellulosic material with remarkable antioxidant activity (Ramírez Tapias et al., 2022). Therefore, this cellulosic material could be used to develop biodegradable films with promising properties for food protection with high mechanical resistance and antioxidant capacity.

On the other hand, it has been demonstrated in a previous work that the incorporation of small molecules in the polymeric matrix improved the functionality of the materials based on the Kombucha tea by-product (Ramírez Tapias et al., 2020). Plasticisers are non-volatile and low-molecular-weight molecules that when incorporated into the polymeric network increased their flexibility and decreased the inherent brittleness of biopolymers-based films (Coma et al., 2019). In addition, plasticisers change the mechanical and thermal properties of the polymeric matrix by reducing intermolecular forces and increasing the space and the mobility of polymer chains, which decreases elastic modulus and glass transition temperature (T_g) (Coma et al., 2019; Montoille et al., 2021). The most commonly used plasticisers for biopolymer-based films are polyols, mono-, di- and oligosaccharides (Vieira et al., 2011). In this way, the fermented broth of Kombucha, which is composed of glucose, not hydrolysed sucrose, cellulosic oligosaccharides and organic acids such as acetic, gluconic and glucuronic acids (Gullo et al., 2019; Ramírez Tapias et al., 2022), could be added to a polymeric matrix to reduce cohesive forces between polymer chains and therefore plasticise the material.

In that respect, this work aims to study Kombucha fermentation in yerba mate infusion for optimisation of BC production and its processing for film formulation. The characteristics of filmogenic dispersion were analysed in terms of rheology and particle size distribution. Subsequently, the properties of the films were identified: microstructural, thermal, mechanical, hydration, water vapour permeability, and antioxidant capacity. Furthermore, this study compares the addition of sterilised fermented broth as a natural plasticiser with traditional glycerol plasticisation. Results revealed that phytochemical compounds of yerba mate and metabolic products of SCOBY culture provided plasticising effect and bioactive properties to films. This aspect resulted in a novelty in the field of material science as the addition of synthetic plasticisers was avoided and the same fermentation product was used for this purpose.

Materials and methods

Reagents

Herbal bags of yerba mate La Tranquera (J. Llorente and Cía S.A., Misiones, Argentina), black tea (Hierbas del Oasis S.R.L., Buenos Aires, Argentina), and food-grade sucrose from Ledesma S.A., (Buenos Aires, Argentina) were purchased in a local market. Analytical grade salts used for the preparation of saturated solutions were purchased from Merck (Darmstadt, Germany). Silica gel was obtained from Biopack (Buenos Aires, Argentina). Analytical grade reagents: ABTS (2,29- azinobis-(3-ethylbenzothiazoline-6-sulfonic acid)), potassium persulfate and DNS (3,5-dinitrosalicylic acid) were obtained from Sigma-Aldrich (St. Louis, MO, USA).

Kombucha fermentation and experimental design

The native culture of Kombucha tea LOMCEM MKO1 was used as the starter culture. This stock culture was prepared and maintained at static conditions at 22 °C and subcultured periodically (21–28 days) in liquid medium based on black tea (4 g/l) and sucrose (100 g/l). After 21 days, the stock Kombucha culture containing $6.0 \pm 0.5 \times 10^6$ colony-forming units per ml ($CFU \cdot ml^{-1}$), was used to inoculate the yerba mate infusion using a volume relation of 1:5 (inoculum:infusion).

The infusion was prepared using 6 g/l of yerba mate in water at 80 °C for 10 min, afterwards, the herbs were separated from the liquid and sucrose was dissolved (100 g/l). The inoculation was carried out at 22 °C to a final volume of 1.5 l This preculture was maintained statically in 3 l glass vessels covered with a cellulose cloth for 21 days (Ramírez Tapias et al., 2022). Subsequently, it was used as the inoculum of a new batch of Kombucha fermentation developed in 300 ml flasks. Factorial experimental design 3^2 was carried out; the evaluated factors were culture volume (ml) and initial sucrose concentration (g/l), using 3 levels of each factor at values of 50, 150 and 250 ml and 20, 100 and 200 g/l, respectively. Response variables were broth pH, film production (g/l), soluble solids (% d.m.), total sugar consumption (g/l), and yield conversion (g/g). Additionally, the native floating films obtained were conditioned according to a previously published procedure (Ramírez Tapias et al., 2022) to study their mechanical performance. Overall, 9 treatments were evaluated in triplicate and response variables were analysed after 21 days. Treatment 5 was a control equivalent to the previous kinetic study (Ramírez Tapias et al., 2022). The treatment that maximised cellulose production with high mechanical performance was selected for scale-up and film formulations.

Scale up of Kombucha cultivated in yerba mate

Once selected best culture conditions based on factorial experimental design, the process was scaled up to 10 × . The total volume of the vessel was 0.3 l scaled to 3 l. It was selected the geometrical parameter based on the ratio of vessel diameter and culture volume height (D/H) (Catapano et al., 2009). Results were validated regarding cellulose production (g/l) and yield conversion (g/g).

Filmogenic dispersions and preparation of films

For film preparation, the wet cellulosic discs were grinded with a blender and filtered in vacuum using a Buchner funnel with filtration paper to remove the water excess. The amount of dry matter of the grinded and filtered material was determined using a small portion of it. The wet material was used for the preparation of film-forming dispersions of 1% d.m. of the cellulosic by-product in distilled water, using the value of the amount of dry matter previously measured. Dispersions were firstly homogenised at 15,000 rpm for 5 min with an Ultraturrax T-25 (IKA, Germany). Then, they were subjected to ultrasonic homogenisation (VCX-750, Sonics and Materials, Inc., USA) at 80 W for 15 min. These processes were carried out twice (Ramírez Tapias et al., 2020). With the purpose of study the effect of plasticiser on film properties, glycerol and solids from the fermented Kombucha broth were compared. Pure glycerol was added to dispersions at levels of 0% (unplasticised sample) and 25% respect to the dry weight of the cellulose in the dispersion. After the addition of glycerol, the dispersion was stirred for 15 min at room temperature. For the incorporation of the solids from the fermented Kombucha broth instead of glycerol, the dispersions were prepared by replacing the distilled water with a dilution of the sterilised fermented broth. This dilution was carried out in such a proportion that the final dispersion contained 25% d.m. of the fermented broth respect to the dry weight of the cellulose. This dispersion was subjected to the

same physical homogenisation treatments as the control dispersion.

To obtain films of thicknesses close to 0.1 mm, 40 g of dispersion was placed in each plastic Petri dish of 86 mm diameter. Evaporation of water was done at 37 °C and 40% relative humidity (r.h.) by casting in a ventilated oven (Sanyo MOV 212F, Japan) until the remaining water content of the films was between 10 and 15%. Then, films were stored at 22 °C and 43% r.h.

Rotary rheology and particle size distribution of filmogenic dispersions

Flow curves were obtained through rotational experiments in a controlled strain AR-G2 rheometer (TA Instruments, Delaware, USA) using a flat plate geometry of 40 mm diameter and 1 mm of gap space. All measurements were performed at 22 °C in triplicate using 1 ml of filmogenic dispersions. Shear stress τ (Pa) as a function of the deformation rate γ (s^{-1}) was measured and curves were adjusted with the Herschel–Bulkley model shown in Eq. (1):

$$\tau = \tau_0 + K\,\gamma^n \quad (1)$$

were τ_0 (Pa) is the threshold shear stress that represents the maximum value of τ for a strain rate equal to zero, K the fluid consistency index, and n the flow behaviour index indicating the deviation to Newtonian flow type ($n>1$ dilating and $n<1$ pseudoplastic).

The particle size distribution (PSD) was obtained by static light scattering (SLS) using a Malvern Mastersizer 2000E analyser equipped with a Hydro 2000MU wet dispersion unit (Malvern Panalytical Ltd; Worcestershire, UK). The optical parameters used to obtain the PSD were the refractive index of the dispersant 1.33 and the refractive index of the particles 1.61 (Niskanen et al., 2019). Particle sizes were expressed as the De Brouckere volume-moment mean diameter ($D_{4,3}$), Sauter surface-moment mean diameter ($D_{3,2}$), and the 90th volume and surface percentiles ($d(0.9)_v$ and $d(0.9)_s$, respectively).

Visual appearance and microstructural characterisation by scanning electron microscopy (SEM) of the films

The evaluation of the appearance of the films, the Cielab coordinates were measured using a Konica Minolta CR400 spectrophotometer (Tuscaloosa, NJ, USA) with illuminant C and observer of 2° according to CIE 1931 standard. The Cielab colour space expresses the lightness, red/green intensity, and yellow/blue intensity, as L*, a*, and b* values, respectively. The colour change ΔE was also calculated through Eq. (2):

$$\Delta E = \sqrt{(L^* - L_o)^2 + (a^* - a_o)^2 + (b^* - b_o)^2} \quad (2)$$

where, L_o, a_o and b_o are the coordinates corresponding to the blank (white calibration plate CR-A44), against the films were compared to determine the colour change owing to each herbal infusion type.

Film thickness was measured with a digital micrometre (± 0.001 m; 3109-25-E, Insize Co., China) using an average of 10 values for each specimen.

The microstructure of films was analysed at high vacuum by using a scanning electron microscope Carl Zeiss NTS–SUPRA. The surfaces (8 kV and magnification × 500) and cross sections (8 kV and magnification × 3000) were studied.

Fourier-transformed infrared spectroscopy analysis (FT-IR)

Infrared spectra of the BC formulated films were determined using a Fourier-Transformed Infrared Analyser (Affinity-1, Shimadzu Co., Japan) equipped with an attenuated total reflectance diamond module (GladiATR, Pike Technologies, USA). Spectra were analysed in the range of 4000–400 cm^{-1} as an average of 45 scans with 4.0 cm^{-1} resolution and Happ-Genzel apodization. The background was set before each test and the spectra were obtained in duplicate.

Differential scanning calorimetry (DSC)

DSC thermograms of the films were measured to understand the thermal behaviour of the films and determination of its relevant thermal events. A Differential Scanning Calorimeter (TA Instruments Q200, Delaware, USA) was used in the range of −80 to 170 °C, with a previous equilibration step at −80 °C for 5 min, and then, the temperature was increased at 10 °C min^{-1}. The modulated procedure was carried out at +/- 1 °C every 40 s. Approximately 7 mg of the sample was placed into Tzero® aluminium pans and sealed with hermetic lids. The samples were equilibrated at 22 °C and 0% r.h. (dehydration in silica gel) and glass transition temperatures (T_g) were determined using TA Universal Analysis software (v4.5, TA Instruments, USA). Experiments were performed in duplicate.

Thermogravimetric analyses (TGA)

Mass loss in samples as a function of temperature was registered in a TA Instruments Q-500 (Delaware, USA) thermos-balance. Films samples were previously placed in a desiccator to be hydrated in equilibrium at 90% r.h. using a saturated salt solution of $BaCl_2$. Approximately 8 mg of each sample were weighed in a platinum pan and heated from 25 to 110 °C at 1 °C min^{-1}, to analyse the loss of hydration water. Then, to study the thermal degradation, film samples were heated from 110 to 800 °C at 20 °C min^{-1}. Experiments were carried out in duplicate under a nitrogen atmosphere (flow rate 60 ml min^{-1}). The temperature at the maximum degradation rate was determined from the maximum of the derivative of the mass loss respect to temperature.

Mechanical properties

Uniaxial tensile tests of native cellulosic films obtained from the 3^2 experimental design and formulated films obtained from filmogenic dispersions, were performed with a Universal Testing Machine (TC-500 II-Series, Micrometric, Argentina) equipped with a 30 kgf cell. The tests were carried out at 5 mm/min using probes of 50 mm × 10 mm, the effective distance between jaws was 25 mm. Ten probes of each film type (n = 10) were conditioned at 52% r.h. and tested at 22 °C. The elastic modulus E (MPa), maximum tensile strength TS (MPa) and deformation at break ε (%) were calculated from the resulting stress-strain curves according to ASTM D882-97 (1997).

Water sorption isotherms

Water sorption isotherms allow studying the equilibrium water uptake as a function of relative humidity (r.h.) or water activity a_w (a_w =% r.h./100) of the environment. Sorption isotherms of films were determined gravimetrically at 22 °C according to the standard procedure previously described (Coma et al., 2019). Dried samples of films of superficial area of 58 cm^2 were placed in desiccators and equilibrated at different water activities a_w. For this, saturated solutions of LiCl, $MgCl_2$, NaBr, NaCl, and $BaCl_2$ were used to generate conditions of a_w of 0.11, 0.33, 0.57, 0.75, and 0.90, respectively. Dried atmospheres were obtained using silica gel. Samples were periodically weighed using an analytical balance ($\pm 10^{-4}$ g) and the evolution to equilibrium at each moisture condition was monitored until constant weight. The water content h (g of water per g of d.m.) was evaluated as a function of a_w. Experiments were performed in triplicates. Isotherms were fitted using Guggenheim–Anderson–De Boer (GAB) model (Guggenheim, 1966) through Eq. (3):

$$h(a_w) = (Nckaw)/[(1 + (c-1)ka_w)(1 - ka_w)] \quad (3)$$

where N is the monolayer water content (g of water per g of dried mass) related to the number of primary binding sites of water molecules, c is a parameter related to the difference between the chemical potential of

the water molecules in the upper layers and in the monolayer, and k a factor related to the difference between the chemical potential of the water in the pure liquid state and in the upper layers. c can also be interpreted as related to the force of the water-binding to monolayer and k as the capability of water binding to multilayer (Salvay, Colombo, & Grigera, 2003).

Water vapour permeability measurements

Water vapour permeability of films was measured using the cup method described in ASTM-E96-2016 with some modifications (Delgado et al., 2018). Films were sealed on the top of cups containing a saturated salt solution of $BaCl_2$ that provides the highest r.h. of 90%. Test cups were placed in 7 l desiccators maintained at a constant temperature of 22 °C and 10% r.h. provided by a saturated salt solution of NaOH. Therefore, water vapour flux was determined from the weight loss of the cup using an analytical balance ($\pm 10^{-3}$ g). A fan was used to maintain uniform conditions inside the desiccators over the films according to recommendations from previous authors (McHugh, Avena--Bustillo, & Krochta, 1993). Weight loss m (g) versus time t was plotted and when the steady-state (straight line) was reached 36 h further were registered. The experimental water vapour permeability P_w^{exp} was calculated as displayed in Eq. (4) (Delgado et al., 2022):

$$P_w^{exp} = \left(\frac{1}{A}\frac{\Delta m}{\Delta t}\right)\frac{L}{\Delta p_w} \quad (4)$$

where A=2.2 × 10^{-3} m^2 is the effective area of exposed film, $\Delta m/\Delta t$ is the slope of a linear regression of the weight loss versus time, L (m) is the film thickness (10 ± 0.01 × 10^{-5} m in this work), Δp_w=(p_{w2}-p_{w1}) is the differential water vapour pressure across the film, and p_{w2} and p_{w1} are the partial pressures (Pa) of water vapour at the film surface inside and outside the cup, respectively (Delgado et al., 2022). P_w^{exp} is given in units of g s^{-1} m^{-1} Pa^{-1}. Experiments were performed in triplicate.

Film antioxidant activity

The antioxidant capacity of the films was determined according to the spectrophotometric procedure previously described (Re et al., 1999). The ABTS [2,29-azinobis-(3-ethylbenzothiazoline-6-sulfonic acid)] radical inhibition was monitored by discolouration. ABTS radical solution ($ABTS^{\bullet+}$) was produced by reacting 7 mM ABTS with 2.45 mM $K_2S_2O_8$ and equilibrating the mixture at room temperature and darkness for 16 h before use. Afterwards, 1 ml of this solution was diluted in ultra-purified water to obtain an absorbence of 0.70 ± 0.02 at 734 nm. Then 5 mg of the film was placed in Eppendorf tubes and 1 ml of $ABTS^{\bullet+}$solution was added. The absorbence at 734 nm was measured at different times (0.25, 0.5, 1, 2, 3, 4, 5 and 8 min) to record the discolouration of the sample. Antioxidant capacity was determined by the percentage of radical inhibition (*%RI*) using Eq. (5):

$$\%\ RI = \frac{0.70 - Sample\ Absorbance\ at\ 734\ nm}{0.70} \times 100 \quad (5)$$

The percentage of radical inhibition of samples as a function of time t,%RI(t), was fitted with a first-order kinetics model (Cantor & Schimmel, 1980), using a biexponential growth function, as displayed in Eq. (6):

$$\%\ RI\ (t) = \%RI_1[1 - exp(-t/\tau_1)] + \%RI_2[1 - exp(-t/\tau_2)] \quad (6)$$

where, $\%RI_1$ and $\%RI_2$ are the percentage of radical inhibition related to inhibition processes 1 and 2, respectively; and τ_1 and τ_2 are the time constant for processes 1 and 2, respectively. The percentage of radical inhibition at equilibrium$\%RI_\infty$ was calculated as $\%RI_\infty = \%RI_1 + \%RI_2$, and the mean time constant τ for the inhibition process was obtained as $\tau = (\%RI_1/RI_\infty)\tau_1 + (\%RI_2/RI_\infty)\tau_2$. Experiments were performed in triplicate at 22 °C.

Statistical analyses

Statistical analyses were performed using Statgraphics centurion 18 (Statgraphics Technologies, Inc.). The data were subjected to the analysis of variance and multiple comparison tests (Tukey test). Differences were considered to be significant at p-value < 0.05.

Results and discussion

Kombucha fermentation and experimental design

The kinetics of Kombucha fermentation in yerba mate was previously studied for 30 days and the film production reached its maximum value of 6.9 ± 0.4 g/l after 21 days (Ramírez Tapias et al., 2022). This time was selected for analysis of the factorial experimental design 3^2. Table 1 shows the evaluated conditions and their effects on SCOBY fermentation parameters using yerba mate.

The infusion of yerba mate provided nutrients such as nitrogen, vitamins and minerals. The main carbon source was sucrose added at values of 20, 100 and 200 g/l, and after inoculation, total sugar content reached 28.2 ± 1.8, 113.6 ± 7.1 and 212.7 ± 6.2 g/l, respectively. The pH value was 4.25 at the initial time and dropped to less than 2.96 after 21 days as a result of sugars oxidation to organic acids and carbon dioxide by AAB and yeasts (Gullo et al., 2017; Laavanya et al., 2021). Regarding film production, both evaluated factors were statistically significant (p-value < 0.001). A lower level of volume and higher sucrose content favoured the formation of the film, and the maximum production was 36.2 g/l for treatment 3 (Table 1). Related to sugar consumption, evaluated factors were statistically significant (p-value < 0.001) and means comparisons by sucrose concentration demonstrated no significant differences for 100 and 200 g/l. Treatments with 20 g/l of sucrose, resulted in a consumption near to 20 g/l, which represented more than 70% of carbohydrate consumption (regarding the initial amount of 28.2 ± 1.8 g/l). By culture volume, treatments with 50 ml favoured the highest sugar consumption and there were no significant differences between 250 and 150 ml. Therefore, treatments 2 and 3 revealed maximum sugar consumption in a mean of 67.4 g/l, a consumption of 60% and 32% of the available carbon and energy source, respectively. Analysis of soluble solids (% d.m.) after 21 days of fermentation, evidenced that a higher level of sucrose content resulted in a higher soluble matter, mostly attributed to residual sugars in the fermentation broth. Since sugar consumption was similar between treatments 2 and 3, the residuals at the end of fermentation were 4.5 and 14.4% d.m., respectively. So, slight differences in total soluble solids reported in Table 1 could be attributed to polyphenols from yerba mate (Butiuk et al., 2021b) and SCOBY metabolic products such as proteins and organic acids, mostly acetic, gluconic and glucuronic (De Filippis et al., 2018). Then, yield conversion (g/g), as the relation of film production with substrate consumption, resulted in significantly superior for treatments with 200 g/l, and the maximum of 0.53 g/g was achieved in treatment 3 (Table 1).

Sucrose content as the main carbon and energy source was a determining factor of fermentation. The lowest availability of sugars resulted in poor film production, the highest level of sucrose was excessive, and the intermediate level of 100 g/l provided the total sugars of the microbial community needed for its biochemical dynamics, evidenced in residual sugars and 19.4 g/l of film production. Regarding culture volume, this factor was directly related to oxygen availability, which is increased in the liquid-air interface. As AAB are strictly aerobic and cellulose production is favoured under static conditions (Gorgieva & Trček, 2019; Laavanya et al., 2021), a higher culture volume represented less oxygen transfer. Therefore, 50 ml of culture volume resulted in a high oxygen availability with enough surface area for mass transfer.

Fig. 1 depicts the integrated results of fermentation parameters and mechanical behaviour of the native films generated at the surface of the liquid beverage for treatments with 50 ml of culture media. At 200 g/l of

Table 1
Matrix of full factorial experimental design 3^2 for fermentation parameters of Kombucha SCOBY cultivated in yerba mate during 21 days at 22 °C and static conditions in 300 ml flasks varying culture volume (ml) and sucrose content (g/l) as studied factors.

Treatment	Factors		Fermentation parameters				
	Volume (ml)	Sucrose (g/l)	pH	Film production (g/l)	Sugar consumption (g/l)	Soluble solids (% d.m.)	Yield (g/g)
1	50	20	2.5 ± 0.04	7.0 ± 1.2	22.1 ± 5.2	1.8 ± 0.5	0.32 ± 0.09
2	50	100	2.24 ± 0.03	19.4 ± 1.5	65.9 ± 3.9	6.0 ± 1.9	0.29 ± 0.05
3	50	200	2.21 ± 0.02	36.2 ± 2.9	68.8 ± 6.4	15.6 ± 2.0	0.53 ± 0.05
4	150	20	2.81 ± 0.03	1.5 ± 0.1	19.6 ± 6.2	2.5 ± 0.6	0.08 ± 0.03
5	150	100	2,49 ± 0.03	6.7 ± 0.4	32.4 ± 5.6	8.1 ± 3.4	0.21 ± 0.04
6	150	200	2.45 ± 0.02	13.6 ± 2.3	28.2 ± 8.1	19.3 ± 1.4	0.48 ± 0.08
7	250	20	2.96 ± 0.02	1.1 ± 0.1	18.7 ± 1.1	2.1 ± 0.2	0.06 ± 0.01
8	250	100	2.66 ± 0.06	2.9 ± 0.1	34.9 ± 7.0	9.7 ± 0.8	0.08 ± 0.04
9	250	200	2.61 ± 0.05	9.2 ± 2.3	28.8 ± 4.9	18.4 ± 0.9	0.32 ± 0.09

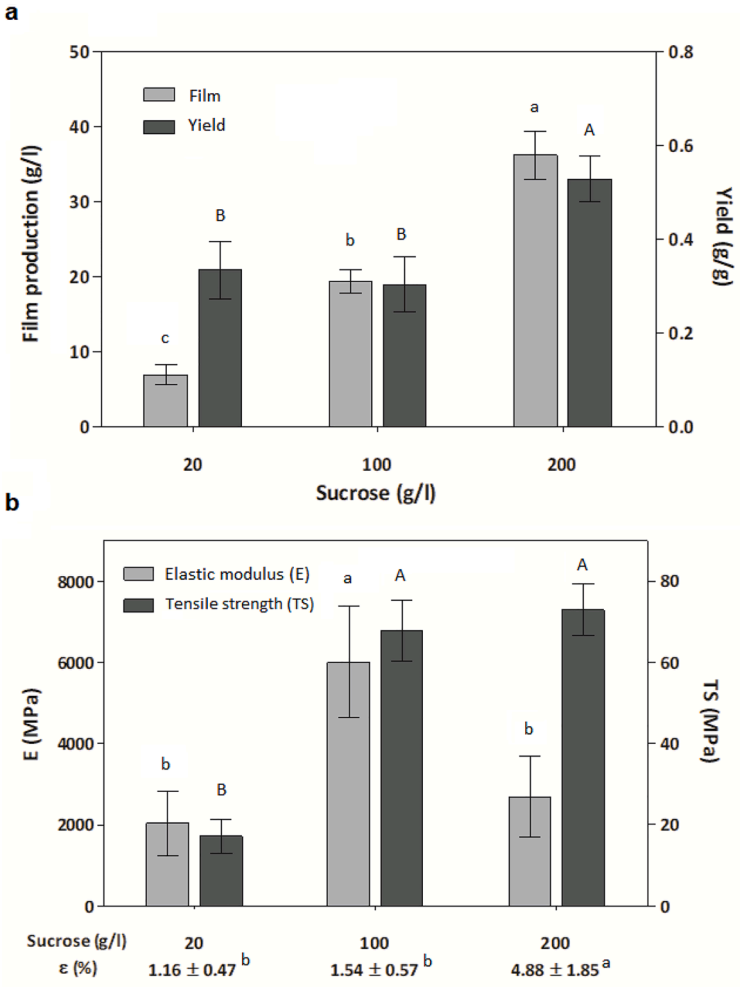

Fig. 1. Kombucha fermentation in 50 ml of yerba mate infusion with the addition of 50, 100 and 200 g/l of sucrose (treatments 1, 2 and 3). a) Film production (g/l) and yield (g/g). b) Mechanical parameters of the native film, generated at the surface of the liquid beverage, for treatments with 50 ml of culture media: elastic modulus *E* (MPa), ultimate tensile strength *TS* (MPa) and deformation at break ε (%).

sucrose (treatment 3), film production and yield conversion of sugars to the polymeric film were maximised, in contrast to treatment 2 with 100 g/l, which performed better for uniaxial tensile assay.

Cultures with 50 ml improved results of the fermentation parameters, especially those with higher availability of sugars (Fig. 1a). Regarding mechanical properties, these treatments produced films with significant performance. With 20 g/l of sucrose, the films demonstrated lower resistance (Fig. 1b), probably due to a limited carbon supply that produced shorter and weaker cellulose filaments. Treatment 2 resulted in the highest elastic modulus of 5996 MPa and 68 MPa of tensile strength, statistically equivalent to 73 MPa observed in treatment 3 (p-value < 0.005) (Fig. 1b). The tensile strength of cellulose films could be associated with sugars consumption probably allowing a high degree of polymerization (Campano et al., 2016). There were no significant differences in consumption between treatments 2 and 3, which resulted in similar tensile strength. In treatment 3, elastic modulus decreased and deformation at break was higher due to additional plasticisation provided for soluble solids mostly residual reducing sugars.

In summary, 50 ml of culture volume and 100 g/l of sucrose (treatment 2) resulted in favourable conditions of sugars and oxygen supply to

produce cellulose with high mechanical resistance. Treatment 2 allowed 19.4 g/l of film production, 2.9 fold higher compared to previously reported results and preserving the mechanical performance (Ramírez Tapias et al., 2022). Thus, it was evidenced a process improvement with a notable reduction of cost production by less volume of growth medium requirement.

Scale up of Kombucha cultivated in yerba mate

Criteria applied for bioreactor selection are focusing on mass transfer and mixing and those considering mechanical damage (Catapano et al., 2009), so static cultures with a large surface promote cellulose production and prevent shear stress to cells during nanofibers exportation.

In static cultivation, the surface area is directly linked to the availability of oxygen in the growth medium in the form of dissolved oxygen (Blanco Parte et al., 2020). The aeration condition determined by the surface/volume (S/V) ratio is an important factor affecting bacterial cellulose synthesis, a larger culture area provides better surface aeration (Gullo et al., 2017), thus increasing the dissolved oxygen in the broth that leads to more SCOBY metabolic activity.

Considering that certain criteria found to be optimal on the small scale might be used for the large scale as well, the ratio of vessel diameter and occupied height (D/H) was kept. Table 2 depicts the dimensions of two vessels and the calculated culture volume for scaled-up Kombucha fermentation that required 600 ml of yerba mate infusion with sucrose at 100 g/l. Therefore, the scale-up by vessel size was 10X but by culture volume was 12 × .

After 21 days of cultivation, the fermentation parameters were quantified to validate the scaled-up process. Film production and sugar consumption was 20.47 ± 1.6 g/l and 68.6 ± 2.4 g/l, respectively, and these results implied a yield conversion of 0.30 ± 0.05 g/g. The film production (dry matter) was 12.28 g/vessel by scale-up, 12.66 fold higher compared with the optimised result (treatment 2: 0.34 g/flask). It demonstrated satisfactory performance of the scaled-up process, which prioritised the surface of oxygen transfer to the microbial community.

Gullo et al. (2017) studied the effect of the S/V ratio for the cultivation of *Komagataeibacter xylinus* K2G30, the 0.23 cm^{-1} condition was chosen according to the highest BC production, yield and productivity of 19.64 g/l, 0.61 g/g and 1.3 g/l·d, respectively, and the lowest by-product formation (gluconic acid). Although the biochemical dynamic is different for bacterial and SCOBY cultures, the results with the same S/V ratio (Table 2) were comparable and suitable for industrial production.

Consequently, the reproducible results of the scaled-up process allowed for obtaining enough material to produce formulated films based on cellulose Kombucha by casting.

Rotary rheology and particle size distribution of filmogenic dispersions

Bacterial cellulose was processed by ultrasonic homogenisation to prepare filmogenic dispersions. Rotary rheology and particle size distribution (PSD) of three different dispersions were studied: without additives (KM), plasticised with 25% glycerol (KM+25% gly) and adding 25% d.m. of the sterilised fermented broth (KM+25% s.c.); the percentage of the plasticisers were respect to the dry weight of the cellulose in the dispersion. Fig. 2a shows the flow behaviour of the filmogenic dispersions and its cellulose particle size distribution (Fig. 2b).

Table 2
Vessels dimension to scale-up kombucha fermentation under static conditions. The D/H ratio was selected as a fixed parameter.

Dimension	Optimised	Scale-up
Vessel volume (cm^3)	300	3000
Vessel high (cm)	9	21
Vessel diameter - D (cm)	6.5	13.5
Culture volume - V (cm^3)	50	600
Occupied height - H (cm)	2	4.2
D/H	**3.2**	**3.2**
Surface - S (cm^2)	32	140
S/V (cm^{-1})	0.64	0.23

The shear stress τ as a function of the deformation rate γ for the different filmogenic dispersions is shown in Fig. 2a. Experimental points were fitted with the Herschel–Bulkley model (Eq. (1)) and the parameters obtained from the fit are displayed in Table 3. The reported values of the statistical parameter R^2 indicate a good acceptance of the fit model for $\gamma<20\ s^{-1}$. For values of $\gamma>20\ s^{-1}$, a radial leakage of dispersion beyond the edges of the plate was observed. This effect was a consequence of the formation of macroscopic aggregates of cellulose fibres produced by the action of flow velocity and expulsed by centrifugal force. For this reason, these experimental values were not considered for the analysis.

All filmogenic dispersions exhibited high values of the threshold shear stress τ_0 (Table 3). Fluids with values of $\tau_0>0$ behave as solids until they exceed the threshold shear stress, then for values of $\tau>\tau_0$ they behave like liquids. These high values of τ_0 were due to the great interaction between the dispersed components (Irgens, 2014). The dispersions studied presented a flow behaviour index $n>1$ corresponding to dilating fluid, which decreased when solids from the culture medium or glycerol were incorporated into the dispersion. On the other hand, the consistency index K increased from 1.1 ± 0.3 Pa s for the dispersion KM to 2.3 ± 0.8 Pa s for the dispersion containing solids from the culture broth (KM+25% s.c.) and finally to 4 ± 1 Pa s for the dispersion containing glycerol (KM+25% gly). These results indicated that the incorporation of solids from the culture medium in the dispersion produced a similar effect to the incorporation of glycerol, increasing the value of K, linked to the apparent viscosity of the dispersion, and decreasing the flow index.

Errors of Herschel–Bulkley parameters were estimated from the fit analysis and statistical parameter R^2 indicates a good acceptance of the model. PSD parameter values were expressed as the mean of three independent determinations (n = 3).

PSD expressed as volume and surface frequency of cellulose dispersions processed by ultrasonic homogenisation are shown in Fig. 2b. PSD exhibited polydispersity and the population was distributed in a broad range of sizes between 3.8 and 1000 μm. Additives in formulations did not significantly affect mean diameters (Tukey test p-value > 0.05) as is shown in Table 3. De Brouckere ($D_{4,3}$) and Sauter ($D_{3,2}$) mean diameters values were 280.5 and 87.5 μm, respectively. The 90% of the particle population based on volume had a diameter less than 639.6 μm and, based on surface this value was 228.1 μm. Significant differences between diameters based on volume and surface could be attributed to polydispersity. Since cellulose is not constituted by particles with relative sphericity, SLS analytical method showed these differences. BC is synthesized by nanofibrils of up to 25 nm in width and 1 to 9 μm in length represent 2000 to 18,000 glucose residues that aggregate into <100 nm wide ribbon-shaped fibrils (Gorgieva & Trček, 2019).

Visual appearance and microstructural characterisation by scanning electron microscopy (SEM) of the films

Formulated films produced by casting were homogeneous with no cracks. Cielab colour parameters of films are shown in Fig. 3: 1A, 1B and 1C.

The films presented lightness $L^* > 65$, they were slightly reddish due to the positive values of a^* ($2 < a^* < 3$) and predominantly yellowish ($17 < b^* < 21$) (Fig. 3). The film without additives and the plasticised with glycerol were similar with no significant differences in the colour change $\triangle E$, with values of 26.8 ± 1.1 and 23.4 ± 2.5, respectively (Fig. 3: 1A and 1C). While the colour change of the film added with the fermented broth was perceptible to the human eye; $\triangle E = 33.2 \pm 0.6$ (Fig. 3: 1B). This yellowness is due to integral cellulosic film produced by fermentation, the casting process produced Maillard reactions which

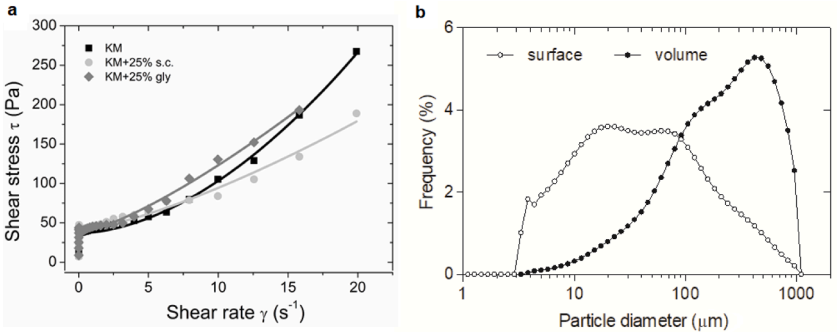

Fig. 2. Characterisation of the filmogenic aqueous dispersions with 1% d.m. of bacterial cellulose. (a) Rotatory rheology analysis by experimental data fitted with the Herschel–Bulkley model (Eq. (1)). Fitted parameters are shown in Table 3. (b) PSD expressed as surface and volume frequency. PSD parameters were not significantly different by the effect of the additives (Table 3).

Table 3
Values of the parameters of flow model and PSD characterisation of filmogenic aqueous dispersions with 1% d.m. of bacterial cellulose. Herschel–Bulkley model parameters fitted for flow curves of Fig. 2. De Brouckere volume-moment mean diameter ($D_{4,3}$), Sauter surface-moment mean diameter ($D_{3,2}$), and the 90th volume and surface percentiles ($d(0.9)_v$ and $d(0.9)_s$, respectively) are shown.

Parameters		Formulations		
		KM	KM+25% s. c.	KM+25% gly
Herschel–Bulkley model	t_0 (Pa)	37 ± 1	40 ± 2	37 ± 1
	K (Pa.s)	1.1 ± 0.3	2.3 ± 0.8	4.0 ± 0.9
	n	1.79 ± 0.09	1.37 ± 0.09	1.32 ± 0.08
	R^2	0.98	0.93	0.96
Particle size distribution	$D_{4,3}$ (μm)	278.9 ± 4.7	284.0 ± 6.1	278.7 ± 9.4
	$D_{3,2}$ (μm)	85.9 ± 2.9	89.0 ± 2.7	87.7 ± 3.5
	$d(0.9)_v$ (μm)	635.3 ± 11.0	646.9 ± 10.3	636.5 ± 22.0
	$d(0.9)_s$ (μm)	223.6 ± 8.9	229.7 ± 6.8	230.9 ± 9.2

occurred between the residual sugars and remaining proteins in addition to coloured compounds from yerba mate (Ramírez Tapias et al., 2022). Besides, the material was not subjected to whitening treatments, such as the use of alkaline solutions (NaOH) for BC purification (Arrieta et al., 2016), since the interest was to keep integral material to preserve the intrinsic bioactivity of the material.

Homogeneity of the films was confirmed by micrographs obtained by SEM of the surfaces (Fig. 3: 2A, 2B and 2C), they exhibited homogeneous surfaces with a continuous matrix with no faults or punctures. The plasticised film KM+25% gly was smoothest (Fig. 3: 1C), KM and KM+25% s.c. evidenced some roughness (Fig. 3: 2A and 2B). The cross-section of the unplasticised film demonstrated fibrils arranged in stacked layers of BC (Fig. 3: 3A). The addition of solids from the fermented broth and glycerol, turned the cross-section more uniform (Fig. 3: 3B and 3C). These differences in rugosity and uniformity were probably due to the interactions by hydrogen bonds of small molecules (glycerol and solids from the fermented broth) that promote cohesion and plasticisation.

Fourier-transformed infrared spectroscopy analysis (FT-IR)

The spectra of the films are shown in Fig. 4. The spectra were normalised to the polysaccharide representative signal at 1030 cm^{-1} for standardised comparison. These spectra showed similarity to those obtained previously for the native film from Kombucha cultured on yerba mate (Ramírez Tapias et al., 2022).

In the range between 3000 and 3600 cm^{-1}, the peak at 3340 cm^{-1} was associated with the stretching vibrations of hydroxyl groups (-OH) of water and polysaccharides (Pakoulev et al., 2003). The range between 2800 and 3000 cm^{-1} showed a peak at 2918 cm^{-1} attributed to the symmetrical and asymmetric vibrations of the functional groups methyl CH_3 and methylene CH_2 and C-H, associated with the cellulose matrix (Cerrutti et al., 2016; Ramírez Tapias et al., 2022). The peaks at 1720 and 1636 cm^{-1} were due to the presence of polyphenols and the bending of the (-OH) of the absorbed water molecules (Gullón et al., 2018; Medina Jaramillo et al., 2016; Ramírez Tapias et al., 2022) they presented the lowest absorbence for KM+25% gly film. As polyphenols are the major components of yerba mate, these signals had a higher absorbence in the KM+25% s.c. film.

In the range of 1200–1500 cm^{-1}, it was evidenced the stretching of the C=O bond due to the presence of remaining organic acids produced during the fermentation of Kombucha, such as acetic acid, gluconic and glucuronic acid (Ramírez Tapias et al., 2020). At 1109 cm^{-1} the peak was attributed to the stretching of the C- O and at 1030 cm^{-1} was evidenced the highest absorbence due to the vibrations of carbohydrate rings and secondary groups (C-O-C; C-OH), confirming the presence of glycosidic bonds β-1,4 in the polymer. These peaks could be associated with the vibrational movements of the glucose molecules that constitute the cellulose matrix, which is the major component of the films (Cerrutti et al., 2016; Makarem et al., 2019; Sharma & Bhardwaj, 2020).

Thermal properties of films: Thermogravimetric (TGA) and differential scanning calorimetry (DSC) analyses

Fig. 5 shows the thermogravimetric analysis of films that were previously hydrated in equilibrium in an atmosphere at 90% r.h.

The degradation zone up to 110 °C shown in Fig. 5a and b, was attributed to water evaporation or dehydration. As compared to the sample KM, the weight loss of films due to dehydration was increased for the film containing solids from the culture medium (KM+25% s.c.) and is further augmented for the sample plasticised with glycerol (KM+25% gly). This revealed that the initial water content increased for the films containing solids from the culture medium or glycerol. As seen in Fig. 5c, the percentage of retained water was lower in the sample KM+25% s.c. as compared with sample KM, indicating that the addition of solids from the culture medium decreased the force of the water-binding to the matrix. For the film plasticised with glycerol, it was observed that the percentage of retained water decreased sharply up to 40 °C, then remained constant up to 80 °C and finally decreased to 0% at 110 °C. This behaviour suggested that the dehydration process of this sample occurred in two stages. In the first one up to 50 °C, the percentage of retained water was lower than samples KM and KM+25% s.c. This was because the plasticiser incorporated in the film's matrix decreased the attractive force between polymer chains increasing free volume and consequently producing a global increase in hydration and water mobility (Coma et al., 2019; Delgado et al., 2018). However, in the second stage, from 40 °C to about 80 °C, the percentage of retained

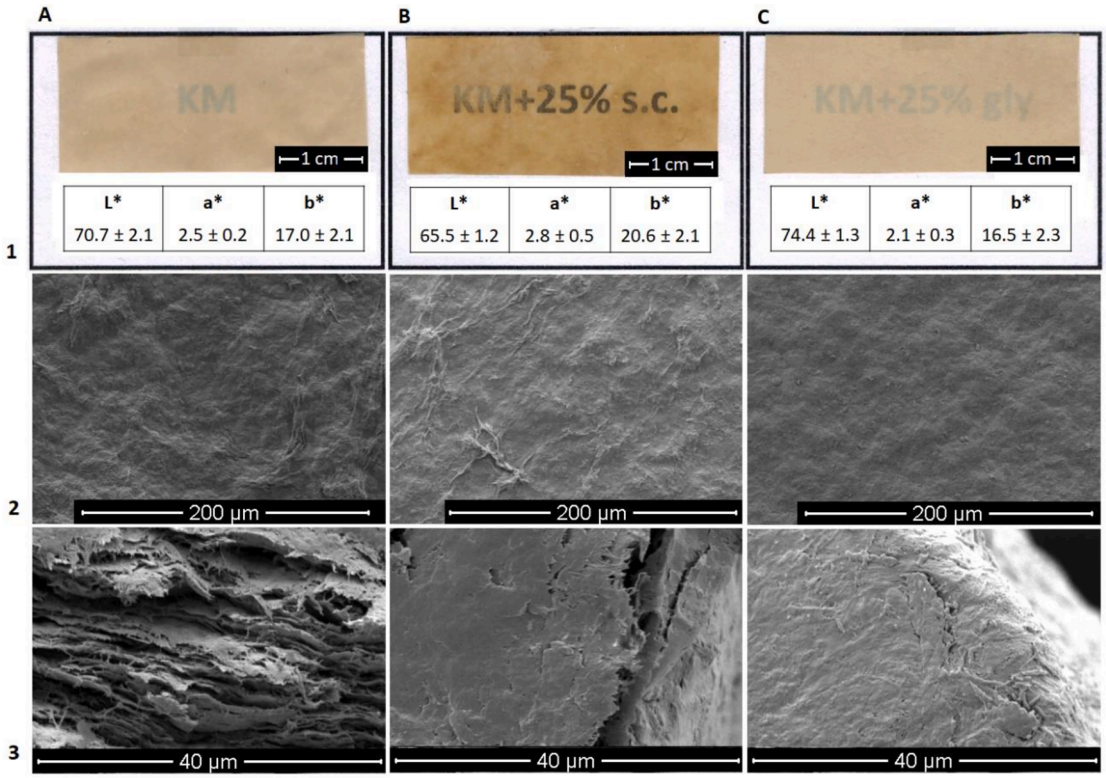

Fig. 3. Visual appearance and SEM microphotographs of films. By columns: A. Unplasticised film (KM). B: Film added with 25% d.m. of culture broth (KM+25% s.c.). C: Film added with 25% d.m. glycerol (KM+25% gly). By rows: 1. Macroscopic visualisation and cielab coordinates. 2: Surface of the films (500 ×). 3: Cross-section (3000 ×).

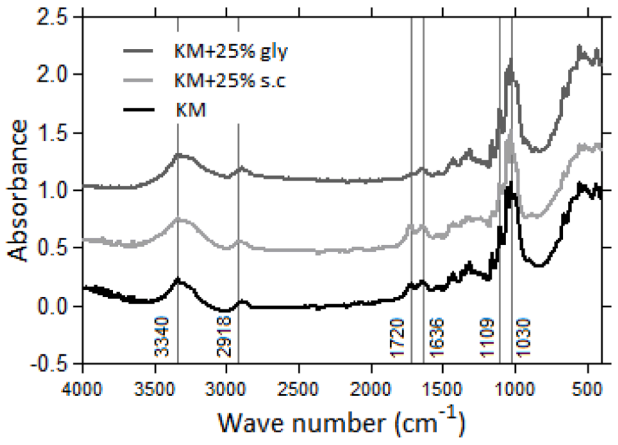

Fig. 4. FTIR spectra in the range of 4000–400 cm^{-1} of the films.

water remained constant at 20%. This could be due to a stronger interaction between the glycerol, the remaining water molecules, and the available (-OH) groups of the cellulose, which could bind in multiple interactions through hydrogen bonds retarding evaporation. Finally, at temperatures above 80 °C, evaporation restarts and is completed at 110 °C.

As can be seen in Fig. 5a and b, at temperatures above 110 °C degradations of samples showed a multistep profile with three different degradation zones. The first degradation zone from 110 °C to 290 °C was related to the degradation of low molecular weight compounds typical of yerba mate, such as polyphenols, xanthines and reducing sugars (Medina Jaramillo et al., 2016; Xia et al., 2015), whose degradation was significant from sample KM+25% s.c. (Fig. 5b) which preserves the components produced in the fermentation. In addition, the degradation of glycerol molecules in the film KM+25% gly occurred in this zone with a maximum decomposition rate at 177 °C (Fig. 5b). A similar degradation of glycerol was observed in water kefir grains-based films (Coma et al., 2019).

The second degradation zone from 290 °C to 400 °C presented a maximum degradation rate at 370 ± 3 °C (Fig. 5b). This pronounced event could be attributed to the thermal degradation of bacterial cellulose (Cerrutti et al., 2016; Ramírez Tapias et al., 2020). Finally, after 400 °C starts the last thermal degradation zone which has been attributed to the degradation of polymeric chains and the six-member cyclic structure, pyran, distinguishing it from the previous decomposition step assigned to the removal of molecular fragments such as hydroxyl and hydroxymethyl groups (Cerrutti et al., 2016; Cheng & Catchmark, 2009).

It could be seen in Fig. 5a an effect due to the plasticisation of the matrix favouring thermal degradation. This is due to the presence of glycerol in the film matrix, which increased chain mobility and exposed polymer chains even more to thermal degradation (Coma et al., 2019). A similar effect could be observed in sample KM+25% s.c., suggesting a plasticiser effect of solids from the culture medium when incorporated in the film matrix. The final residue at 800 °C was affected by the initial quantity of solids from the culture medium or glycerol added to samples (Fig. 5a).

Glass transition temperatures (T_g) of films were studied by DSC experiments with the samples in dry conditions to observe thermal events independently of the water content of films. Table 4 presents the values of T_g of the dehydrated films. The film without additives presented the highest T_g at 9.5 ± 3.0 °C, and it was slightly decreased to 2.4 ± 1.1 °C by the addition of the solids from the fermented broth, meanwhile, glycerol affected drastically the T_g of de material, decreasing the value to −56.1 ± 3.6 °C. This behaviour was attributed to the plasticisation produced by the additives; especially glycerol which decreases the attractive forces between cellulose chains, producing an increase in the

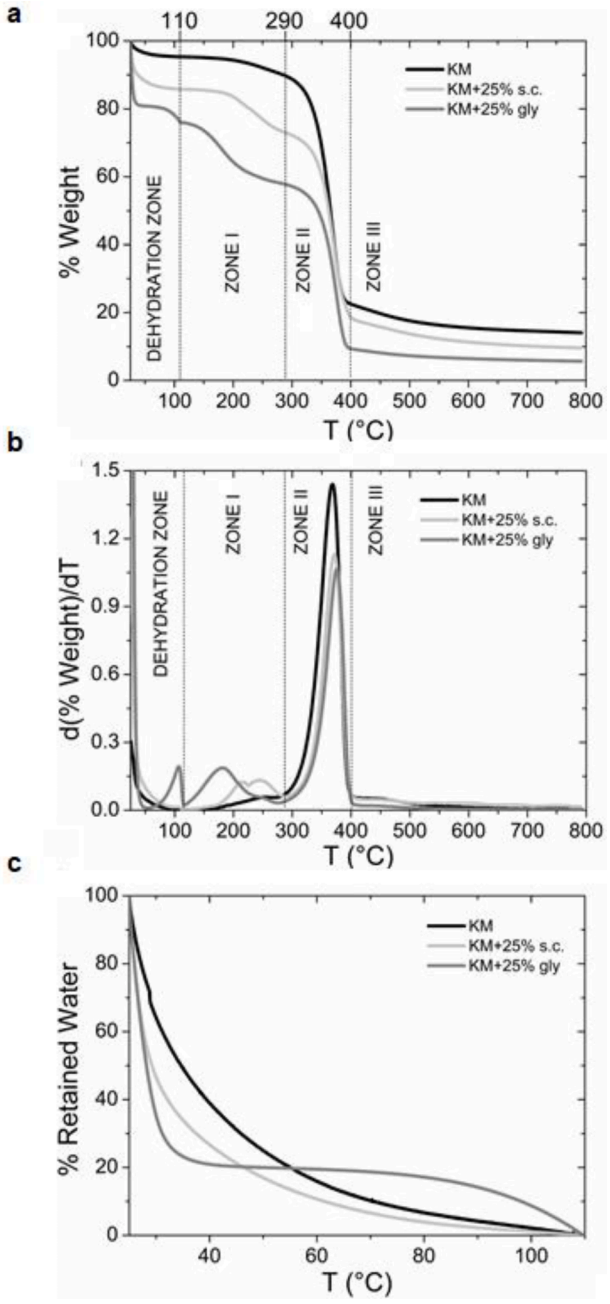

Fig. 5. Thermogravimetric analysis of films: (a) Mass loss. (b) Derivative of mass loss. (c) Percentage of retained water as a function of temperature.

molecular space and mobility favouring the transition from glassy to rubbery state. Small molecules of fermented broth plasticised the films as was demonstrated in a previous report, where films obtained from an intentionally submerged cellulosic disc of Kombucha fermented in black tea showed a T_g of 3 °C, which demonstrated a natural plasticisation compared to the T_g of 16 °C of films obtained from the superficial disc (Ramírez Tapias et al., 2020). BC native films produced by *G. xylinus* PTCC 1734 showed a T_g of −33 °C (Hosseini et al., 2018) and commercial microcrystalline cellulose powder with 7% water content presented a T_g of 25 °C (Szcześniak et al., 2008). Crystalline macromolecules like cellulose could present different values of T_g because it is affected by factors such as polymerisation degree, purity, crystallinity index and type of drying process (Hosseini et al., 2018).

Table 4
Parameters of characterisation of formulated cellulose films. Glass transition temperature of dehydrated films (0% r.h.) calculated by DSC. Mechanical parameters: ultimate tensile strength *TS* (MPa), elastic modulus *E* (MPa), and deformation at break *ε* (%). Hydration and experimental water vapour permeability of films. Values of the GAB parameters fitted for the water sorption isotherms of Fig. 6. Water vapour permeability (P_w^{exp}) was expressed in the standard units of 10^{-10} g s^{-1} m^{-1} Pa^{-1}. Values of the parameters for the antioxidant activity kinetics showed in Fig. 7 using the biexponential kinetic model.

Parameters		Formulations		
		KM	KM+25% s. c.	KM+25% gly
Glass transition temperature	*Tg* (°C)	9.5 ± 3.0 [a]	2.4 ± 1.1 [b]	- 56.1 ± 3.6 [c]
Mechanical parameters	*TS* (MPa)	39.9 ± 9.5 [a]	25.1 ± 4.1 [b]	20.3 ± 6.9 [b]
	E (MPa)	1711.0 ± 498.9 [a]	997.8 ± 217.7 [b]	734.6 ± 206.1 [b]
	ε (%)	5.55 ± 0.95 [b]	6.91 ± 2.34 [a]	6.11 ± 1.76 a
GAB parameters from water sorption isotherms	*N* (g per g)	0.031 ± 0.003	0.077 ± 0.009	0.066 ± 0.007
	C	22 ± 5	0.84 ± 0.08	2.7 ± 0.9
	K	0.94 ± 0.02	0.93 ± 0.03	0.99 ± 0.03
	$h_{90\%hr}$ (g per g)	0.20 ± 0.01 [c]	0.40 ± 0.02[b]	0.57 ± 0.02 [a]
	R^2	0.992	0.998	0.998
Vapour permeability	P_w^{exp}	2.2 ± 0.1 [c]	2.9 ± 0.1 [b]	3.3 ± 0.1 [a]
Antioxidant activity: kinetics parameters	$\%RI_\infty$	95 ± 4	99 ± 8	95 ± 7
	τ (min)	1.6 ± 0.9	2.4 ± 0.4	1.6 ± 0.5
	τ_1(min)	0.23 ± 0.01	0.28 ± 0.04	0,19 ± 0.051
	τ_2 (min)	3.9 ± 0.8	6.2 ± 0.9	2,7 ± 0,8
	$\%RI_1$	60 ± 2	63 ± 3	43 ± 4
	$\%RI_2$	35 ± 2	36 ± 2	52 ± 4
	R^2	0.999	0.996	0.995

Errors in the GAB model and Antioxidant activity kinetics parameters were estimated from the fit analysis.
$h_{90\%\ r.h.}$ was the equilibrium value of the hydration at 90% r.h.
The reported values of the statistical parameter R^2 indicated a very good acceptance of the model.
Different letters in the same row indicate statistically significant differences ($p < 0.05$).

Mechanical properties

Uniaxial tensile tests of formulated films were performed at 22 °C and 52% r.h. The maximum tensile strength *TS* (MPa), elastic modulus *E* (MPa), and deformation at break *ε* (%) were calculated from the experimental stress-strain curves, the values are shown in Table 4. The unplasticised film showed maximum mechanical resistance with *TS* and *E* values of 39.9 and 1711.0 MPa, respectively. In contrast to native films (Fig. 1b), the formulated reduced these parameters by the effect of sonication. The strong cellulosic matrix produced by bacteria was affected by the size reduction and homogenisation processes of film formulation, reducing linkages between chains and their intermolecular interactions (Jia et al., 2018; Vieira et al., 2011). This formulation process raised deformation at break values due to the high mobility of the polymers. The additives produced a reduction of *TS* and *E* while augmenting the ε, with no statistical differences between the effect of glycerol and fermented broth. This behaviour showed a similar effect by both additives that changed the spacing between molecules, decreasing interpolymer interactions, and allowing flexibility. Addition of solids from the fermented broth evidenced a mechanical performance with 25.1 MPa of *TS*, 997.8 MPa of *E*, and 6.91% of *ε* (Table 4). These results are relevant due to the natural plasticisation provided by the fermented product that preserves the bioactivity of the film, mechanical performance and thermal properties. This could be an advantage for film development since it is possible to avoid additional plasticiser

representing a reduction in the cost of the process.

There is a wide range of reported data for the mechanical properties of BC in other studies; differences may be attributed to film formulation techniques. Reports of films obtained by compression and casting of the cellulosic dispersion (Ramírez Tapias et al., 2020; Rozenberga et al., 2016) have shown different values for these mechanical parameters. Indeed, film fabrication methodologies allow the design of nanostructured materials with high mechanical performance.

Hydration and water vapour permeability

Water sorption isotherms of films are shown in Fig. 6. Experimental points were fitted with the GAB model done by Eq. (2) and fitted parameters are displayed in Table 4.

All of the isotherms showed a slight increase in the hydration water content at low values of a_w, and a sharp increase for a_w>0.6. In general, this behaviour of sorption isotherms is common for most hydrophilic films made from biopolymers (Delgado et al., 2022). This shape of sorption isotherms suggested the existence of a small amount of water directly bound to the polymeric matrix, forming the hydration monolayer. Then, most of the hydration water molecules were forming multilayers and were indirectly bound to the polymeric matrix. Therefore, hydration water molecules in biopolymeric materials are liable to be moved by the diffusion mechanism through a water vapour pressure gradient (Delgado et al., 2022; Delgado et al., 2018a).

It was observed from Fig. 6 that the amount of hydration water in the film was increased with the incorporation of solids from the culture medium (KM+25% s.c.) and is further augmented for the samples plasticised with glycerol (KM+25% gly). This increase in hydration occurred without changing the shape of the isotherm. Similar behaviour was observed for most of the biopolymer-based films when plasticising agents were incorporated (Coma et al., 2019; Coupland et al., 2000; Delgado et al., 2018a; Ramírez Tapias et al., 2020). Therefore, the incorporation of solids from the culture medium in the films produced an effect on the hydration similar to that of plasticisers.

The isotherm of KM film without the incorporation of plasticisers agents (Fig. 6) exhibited a similar shape to the isotherm of the unprocessed native film produced in the fermentation of Kombucha in yerba mate infusion (Ramírez Tapias et al., 2022). However, the unprocessed native film presented a hydration equilibrium value at 90% r.h. of 0.16 ± 0.01 g H_2O per g d.m. (Ramírez Tapias et al., 2022), which was minor as compared with the KM film ($h_{90\%rh}$ = 0.20 ± 0.01 g H_2O per g d.m., as seen in Table 4). This suggested that the processing of native material

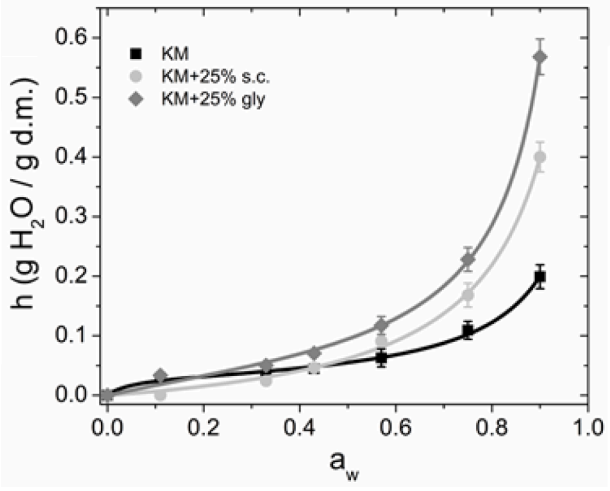

Fig. 6. Water sorption isotherms of the formulated films of bacterial cellulose. Experimental data were fitted with the GAB model. Fitted parameters are shown in Table 4.

altered the polymer network exposing more hydrophilic groups available for hydration. Moreover, unplasticised films obtained by processing Kombucha by-product of the fermentation in tea infusion presented a hydration equilibrium value at 90% r.h. of 0.54 ± 0.02 g H_2O per g d.m. (Ramírez Tapias et al., 2020). This value of $h_{90\%rh}$ was remarkably larger as compared with the obtained for the unplasticised KM film in this work. This result confirmed previous studies about the important influence of the herbal infusion used for the fermentation on the properties of the by-product (Ramírez Tapias et al., 2022). Furthermore, comparing the isotherm of unplasticised KM film displayed in Fig. 6 with isotherms of other unplasticised biopolymeric films; it could be observed that the hydration of KM films was lower than films based on starch (Bertuzzi et al., 2007), myofibrillar protein (Cuq et al., 1997), yeast cell wall (Peltzer et al., 2018), whole yeast biomass (Delgado et al., 2016) and water kefir grains biomass (Coma et al., 2019).

Table 4 displays the parameters obtained from fitting sorption isotherms with the GAB model. Parameter *N* related to the number of primary binding sites of hydration increased with the incorporation of solids from the culture medium and with the addition of glycerol, while parameter *c* linked to the force of the water-binding to these primary sites decreased with the incorporation of additives in the film. Then, parameter *k* related to the capability of water to be bounded to the multilayer remained constant considering the errors of the parameters obtained. Similar behaviour of GAB parameters with the incorporation of glycerol in the films was observed in films based on whey protein (Coupland et al., 2000) cassava starch (Mali et al., 2005), yeast cell wall (Peltzer et al., 2018), and water kefir grains biomass (Coma et al., 2019).

From the analysis of the water sorption isotherms, it could be concluded that the incorporation of solids from the culture medium acted as a plasticiser in the same way that the addition of glycerol, increasing the amount of hydration water in the monolayer, but decreasing the force of the water-binding to the primary sites of hydration. Both plasticising agents interacted with bacterial cellulose chains by establishing hydrogen bonds with the reactive groups of the polymer. Therefore, these plasticisers incorporated into the film matrix decreased the attractive forces between polymer chains and increased free volume and segmental motions. In this way, the incorporation of solids from the culture medium as well as the addition of glycerol in the film matrix produces a global increase in hydration water content, allowing greater mobility to water molecules, as also described in thermogravimetric studies.

Water vapour permeability of biopolymer-based films is an important property, indicating their ability to control water vapour transport between a system (e.g. food) and its surroundings. It was found in Fig. 3 that film micrographs exhibited a continuous and homogenous matrix, without macropores, faults, or film punctures. These studies indicated that the water transport in the films did not occur through pores but by means of the mechanism of sorption-diffusion-desorption (Delgado et al., 2022; Delgado et al., 2018a; Roy et al., 2000). Therefore, water vapour permeability depends on the hydration or water solubility in the film as well as the mobility of water molecules in the matrix (Delgado et al., 2022).

Experimental water vapour permeability P_w^{exp} was obtained by Eq. (3) and shown in Table 4. It was observed that P_w^{exp} increased with the incorporation of solids from the culture medium (KM+25% s.c.) and is further augmented for samples containing glycerol (KM+25% gly). The effect of plasticisers increasing water vapour permeability was observed in most biopolymer-based films (Bertuzzi et al., 2007; Coma et al., 2019; Delgado et al., 2018b; Peltzer et al., 2018; Ramírez Tapias et al., 2020). Water sorption isotherms and thermogravimetric analysis showed that the increase in the incorporation of solids from the culture medium as well as the addition of glycerol in the films produced a global increase in hydration and greater mobility to water molecules. Consequently, it was expected that the water vapour permeability of films would be increased with the incorporation of both plasticiser agents.

Water vapour permeability of biopolymer-based films deviates

substantially from the ideal behaviour and depends on the experimental conditions such as the differential water vapour partial pressure across the test Δp_w and the thickness L of the film (Delgado et al., 2022). This is because of the strong interaction between the film matrix and the permeant water. Therefore, the comparison of water vapour permeability values of different types of hydrophilic films is difficult, since the water vapour permeability of biopolymer-based films is generally reported as a single value in a particular experimental condition of water pressure gradient and film thickness, which provides limited information. In the present work, experimental water vapour permeability ranged from 2.2 ± 0.1 to 3.3 ± 0.1 10^{-10} g m^{-1} s^{-1} Pa^{-1}. Nevertheless, the order of magnitude of the measured P_w^{exp} for the films studied in this work was similar to films obtained from other biopolymers and measured at the same experimental conditions of the differential water vapour partial pressure across the film Δp_w. However, the different thicknesses reported from these films difficult the comparison between them.

Film antioxidant activity

Oxidative reactions strongly promote food degradation that could be prevented by the development of active packaging with antioxidant activity to improve the stability of sensitive food products (Vilela et al., 2018). The addition of active compounds to film formulations to enhance the antioxidant or antimicrobial properties in food surfaces is the most used methodology to develop these materials (Cottet, Salvay, & Peltzer, 2021; Zhu, 2021). However, antioxidant capacity could be achieved using the integral BC produced by Kombucha fermented in yerba mate (Ramírez Tapias et al., 2022).

The antioxidant activity of films was measured using the ABTS method and the kinetics of the processes were modelled by Eq. (6). Results are shown in Fig. 7 and Table 4.

These results evidenced radical inhibition reactions that occurred in a short period for the three evaluated films and required less than 10 min to reach a value greater than 95% radical inhibition. The kinetics followed biphasic behaviour. Firstly, a fast stage is followed by a slower one, up to the equilibrium. Time constants τ_1 for the fast process and τ_2 for the slow one are shown in Table 4. Firstly, occurs a fast migration of the antioxidant molecules probably due to weak links and subsequently, a slow migration mechanism developed, because of strongly attached related antioxidant molecules. Fast and slow processes contributed to the total percentage of radical inhibition at equilibrium. The film added with glycerol evidenced lower time constants (τ_1: 0.19 and τ_2: 2.7 min) due to higher mobility of the molecules amongst the matrix. Contrary to the film added with solids from the fermented broth that revealed higher time constants (τ_1: 0.28 and τ_2: 6.2 min) probably due to more attached active molecules from fermented broth; however, it demonstrated the highest radical inhibition of 99 ± 8% (Table 4). This exceptional%*RI* value is attributed to polyphenolic compounds (chlorogenic acid) and xanthines (caffeine and theobromine) provided by yerba mate (Butiuk et al., 2021a), which have been recognized as hydrogen donors, acting like a free radical scavenger (Cottet, Salvay, & Peltzer, 2021).

The great importance of this result lies in the fact that was not necessary the addition of two different components to plasticise and provide antioxidant activity to the films, with a natural additive that comes from the same fermentation both effects were achieved.

Conclusion

The community of bacteria and yeasts from Kombucha fermented in yerba mate produces bacterial cellulose with extraordinary mechanical and bioactive properties. The cultures were affected by total sugars availability: the main energy source and cellulose synthesis precursor, and the volume culture: a variable related to the area for oxygen mass transfer. The process was scaled-up 10X preserving the optimised production of 19.4 g/l of cellulose and 0.29 g/g of yield. Homogenisation procedures allow obtaining dispersions for standardised film formulations. Cellulosic dispersions behaved as dilating fluid, and the apparent viscosity was augmented with the addition of solids from the fermented broth and glycerol. Particle size distribution analysis showed a broad range of sizes between 3.8 and 1000 μm, constituted by conglomerates of nanofibrils.

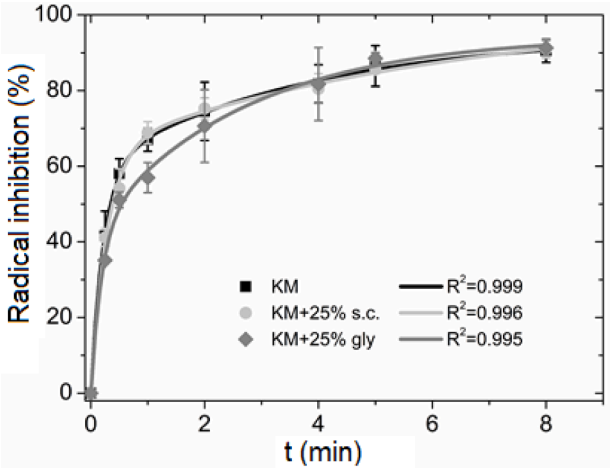

Fig. 7. Antioxidant capacity of formulated cellulose films. Experimental data were fitted with a biexponential function corresponding to a first-order kinetics. Fitted parameters are shown in Table 4.

The formulated films were flexible and exhibited great continuity and homogeneity with the microstructure composed of a cellulosic matrix of nanofibers. Infrared spectroscopy, thermogravimetric analyses, and antioxidant capacity assays indicated the main composition of cellulose with the presence of bioactive compounds from yerba mate that provided a high antioxidant activity. A natural plasticisation was observed by the addition of fermented broth without significant differences from glycerol, a traditional plasticiser. This result is important to decrease or avoid the use of external plasticisers, reducing the cost of film formulation and taking advantage of bioactive molecules with functional properties. The results demonstrated the potential of designing sustainable bioprocess to develop active materials to protect food against oxidation.

Declaration of Competing Interest

The authors declare that they have no known competing financial interests or personal relationships that could have appeared to influence the work reported in this paper.

Data availability

Data will be made available on request.

Acknowledgments

The authors received financial support from Universidad Nacional de Quilmes (UNQ, Argentina) through R&D program PUNQ 990/19 (2019 – 2023). Ramírez-Tapias thanks CONICET for the postdoctoral research scholarship. Di Monte thanks to EVC-CIN (2019) for the engineering student scholarship.

References

Arrieta, M. P., Fortunati, E., Burgos, N., Peltzer, M. A., López, J., & Peponi, L. (2016). Nanocellulose-based polymeric blends for food packaging applications. *Multifunctional polymeric nanocomposites based on cellulosic reinforcements*. Elsevier Inc. https://doi.org/10.1016/B978-0-323-44248-0.00007-9

ASTM D882-97. (1997). Standard test method for tensile properties of thin plastic sheeting. *Annual book of ASTM standards*. Philadelphia: American Society for Testing and Materials.

Bertuzzi, M. A., Castro Vidaurre, E. F., Armada, M., & Gottifredi, J. C. (2007). Water vapor permeability of edible starch based films. *Journal of Food Engineering, 80*(3), 972–978. https://doi.org/10.1016/j.jfoodeng.2006.07.016

Blanco Parte, F. G., Santoso, S. P., Chou, C. C., Verma, V., Wang, H. T., Ismadji, S., et al. (2020). Current progress on the production, modification, and applications of bacterial cellulose. *Critical Reviews in Biotechnology, 40*(3), 397–414. https://doi.org/10.1080/07388551.2020.1713721

Bueno, F., Chouljenko, A., & Sathivel, S. (2021). Development of coffee kombucha containing Lactobacillus rhamnosus and Lactobacillus casei: Gastrointestinal simulations and DNA microbial analysis. *LWT, 142*(January), Article 110980. https://doi.org/10.1016/j.lwt.2021.110980

Burris, K. P., Harte, F. M., Michael Davidson, P., Stewart, C. N., & Zivanovic, S. (2012). Composition and bioactive properties of Yerba Mate (Ilex paraguariensis A. St.-Hil.): A review. *Chilean Journal of Agricultural Research, 72*(2), 268–274. https://doi.org/10.4067/s0718-58392012000200016

Butiuk, A. P., Maidana, S. A., Adachi, O., Akakabe, Y., Martos, M. A., & Hours, R. A. (2021a). Optimization and modeling of the chlorogenic acid extraction from a residue of yerba mate processing. *Journal of Applied Research on Medicinal and Aromatic Plants, 25*(May), Article 100329. https://doi.org/10.1016/j.jarmap.2021.100329

Butiuk, A. P., Maidana, S. A., Adachi, O., Akakabe, Y., Martos, M. A., & Hours, R. A. (2021b). Optimization and modeling of the chlorogenic acid extraction from a residue of yerba mate processing. *Journal of Applied Research on Medicinal and Aromatic Plants, 25*(May), Article 100329. https://doi.org/10.1016/j.jarmap.2021.100329

Campano, C., Balea, A., Blanco, A., & Negro, C. (2016). Enhancement of the fermentation process and properties of bacterial cellulose: A review. *Cellulose (London, England), 23*(1), 57–91. https://doi.org/10.1007/s10570-015-0802-0

Cantor, C. R., & Schimmel, P. R. (1980). *Biophysical chemistry, part 3: The behavior of biological macromolecules*. New York, NY, USA: W.H. Freeman & Co.

Catapano, G., Czermak, P., Eibl, R., Eibl, D., & Pörtner, R (2009). Bioreactor design and scale-up. In P. Eibl, R. Eibl, D. Pörtner, R. Catapano, & G. Czermak (Eds.), *Cell and tissue reaction engineering: Principles and practice*. Berlin Heidelberg: Springer-Verlag.

Cerrutti, P., Roldán, P., García, R. M., Galvagno, M. A., Vázquez, A., & Foresti, M. L. (2016). Production of bacterial nanocellulose from wine industry residues: Importance of fermentation time on pellicle characteristics. *Journal of Applied Polymer Science, 133*(14), 1–9. https://doi.org/10.1002/app.43109

Chakravorty, S., Bhattacharya, S., Bhattacharya, D., Sarkar, S., & Gachhui, R. (2019). Kombucha: A promising functional beverage prepared from tea. *Non-alcoholic beverages: Volume 6. The science of beverages*. Elsevier Inc. https://doi.org/10.1016/B978-0-12-815270-6.00010-4

Cheng, K. C., & Catchmark, J. M. (2009). Effect of different additives on bacterial cellulose production by Acetobacter xylinum and analysis of material property. *Cellulose (London, England), 16*, 1033–1045. https://doi.org/10.1007/s10570-009-9346-5

Coma, M. E., Peltzer, M. A., Delgado, J. F., & Salvay, A. G. (2019). Water kefir grains as an innovative source of materials: Study of plasticiser content on film properties. *European Polymer Journal, 120*(August), Article 109234. https://doi.org/10.1016/j.eurpolymj.2019.109234

Cottet, C., Ramírez-Tapias, Y. A., Delgado, J. F., De La Osa, O., Salvay, A. G., & Peltzer, M. A. (2020). Biobased materials from microbial biomass and its derivatives. *Materials, 13*(1263), 1–26.

Cottet, C., Salvay, A., & Peltzer, M. A. (2021). Incorporation of poly (itaconic acid) with quaternized thiazole groups on gelatin-based films for antimicrobial-active food packaging. *Polymers, 13*(200), 1–21.

Coupland, J. N., Shaw, N. B., Monahan, F. J., Dolores O'Riordan, E., & O'Sullivan, M (2000). Modeling the effect of glycerol on the moisture sorption behavior of whey protein edible films. *Journal of Food Engineering, 43*(1), 25–30. https://doi.org/10.1016/S0260-8774(99)00129-6

Cuq, B., Gontard, N., Aymard, C., & Guilbert, S. (1997). Relative humidity and temperature effects on mechanical and water vapor barrier properties of myofibrillar protein-based films. *Polymer Gels and Networks, 5*(1), 1–15. https://doi.org/10.1016/S0966-7822(96)00026-3

De Filippis, F., Troise, A. D., Vitaglione, P., & Ercolini, D. (2018). Different temperatures select distinctive acetic acid bacteria species and promotes organic acids production during Kombucha tea fermentation. *Food Microbiology, 73*, 11–16. https://doi.org/10.1016/j.fm.2018.01.008

Delgado, J. F., Peltzer, M. A., & Salvay, A. G. (2022). Water vapour transport in biopolymeric materials: Effects of thickness and water vapour pressure gradient on yeast biomass-based films. *Journal of Polymers and the Environment, 30*, 2976–2989. https://doi.org/10.1007/s10924-022-02412-6

Delgado, J. F., Peltzer, M. A., Salvay, A. G., de la Osa, O., & Wagner, J. (2018a). Characterization of thermal, mechanical and hydration properties of novel films based on Saccharomyces cerevisiae biomass. *Innovative Food Science & Emerging Technologies, 48*, 240–247. https://doi.org/10.1016/j.ifset.2018.06.017

Delgado, J. F., Peltzer, M. A., Wagner, J. R., & Salvay, A. G. (2018b). Hydration and water vapour transport properties in yeast biomass based films: A study of plasticizer content and thickness effects. *European Polymer Journal, 99*(November 2017), 9–17. https://doi.org/10.1016/j.eurpolymj.2017.11.051

Delgado, J. F., Sceni, P., Peltzer, M. A., Salvay, A. G., De La Osa, O., & Wagner, J. R. (2016). Development of innovative biodegradable films based on biomass of Saccharomyces cerevisiae. *Innovative Food Science and Emerging Technologies, 36*, 83–91. https://doi.org/10.1016/j.ifset.2016.06.002

Gorgieva, S., & Trček, J. (2019). Bacterial cellulose: Production, modification and perspectives in biomedical applications. *Nanomaterials, 9*(10), 1–20. https://doi.org/10.3390/nano9101352

Guggenheim, E. A. (1966). *Applications of statistical mechanics*. Oxford: Claredon Press, Article 0198553315.

Gullo, M., La China, S., Petroni, G., Di Gregorio, S., & Giudici, P. (2019). Exploring K2G30 genome: A high bacterial cellulose producing strain in glucose and mannitol based media. *Frontiers in Microbiology, 10*(JAN), 1–12. https://doi.org/10.3389/fmicb.2019.00058

Gullo, M., Sola, A., Zanichelli, G., Montorsi, M., Messori, M., & Giudici, P. (2017). Increased production of bacterial cellulose as starting point for scaled-up applications. *Applied Microbiology and Biotechnology, 101*(22), 8115–8127. https://doi.org/10.1007/s00253-017-8539-3

Gullón, B., Eibes, G., Moreira, M. T., Herrera, R., Labidi, J., & Gullón, P. (2018). Yerba mate waste: A sustainable resource of antioxidant compounds. *Industrial Crops and Products, 113*(January), 398–405. https://doi.org/10.1016/j.indcrop.2018.01.064

Hosseini, H., Kokabi, M., & Mousavi, S. M. (2018). Dynamic mechanical properties of bacterial cellulose nanofibres. *Iranian Polymer Journal (English Edition), 27*(6), 433–443. https://doi.org/10.1007/s13726-018-0621-x

Irgens, F. (2014). *Rheology and non-Newtonian fluids* (1st ed.). Switzerland: Springer Cham.. https://doi.org/10.1007/978-3-319-01053-3

Jia, P., Xia, H., Tang, K., & Zhou, Y. (2018). Plasticizers derived from biomass resources: A short review. *Polymers, 10*(12). https://doi.org/10.3390/polym10121303

Laavanya, D., Shirkole, S., & Balasubramanian, P. (2021). Current challenges, applications and future perspectives of SCOBY cellulose of Kombucha fermentation. *Journal of Cleaner Production, 295*, Article 126454. https://doi.org/10.1016/j.jclepro.2021.126454

Makarem, M., Lee, C. M., Kafle, K., Huang, S., Chae, I., Yang, H., et al. (2019). Probing cellulose structures with vibrational spectroscopy. In *Cellulose* (Vol. 26). Netherlands: Springer. https://doi.org/10.1007/s10570-018-2199-z

Mali, S., Sakanaka, L. S., Yamashita, F., & Grossmann, M. V. E. (2005). Water sorption and mechanical properties of cassava starch films and their relation to plasticizing effect. *Carbohydrate Polymers, 60*(3), 283–289. https://doi.org/10.1016/j.carbpol.2005.01.003

May, A., Narayanan, S., Alcock, J., Varsani, A., Maley, C., & Aktipis, A. (2019). Kombucha: A novel model system for cooperation and conflict in a complex multi-species microbial ecosystem. *PeerJ, 2019*(9), 1–22. https://doi.org/10.7717/peerj.7565

McHugh, T. H., Avena-Bustillo, R., & Krochta, J. M. (1993). Hydrophilic edible films: modified procedure for water vapor permeability and explanation of thickness effects. *Journal of Food Science, 58*, 899–903.

Medina Jaramillo, C., Gutiérrez, T. J., Goyanes, S., Bernal, C., & Famá, L. (2016). Biodegradability and plasticizing effect of yerba mate extract on cassava starch edible films. *Carbohydrate Polymers, 151*, 150–159. https://doi.org/10.1016/j.carbpol.2016.05.025

Mokhena, T. C., & John, M. J. (2019). Cellulose nanomaterials: New generation materials for solving global issues. In *Cellulose, 0123456789*. Netherlands: Springer. https://doi.org/10.1007/s10570-019-02889-w

Montoille, L., Morales Vicencio, C., Fontalba, D., Ortiz, J. A., Moreno-Serna, V., Peponi, L., et al. (2021). Study of the effect of the addition of plasticizers on the physical properties of biodegradable films based on kefiran for potential application as food packaging. *Food Chemistry, 360*(May), Article 129966. https://doi.org/10.1016/j.foodchem.2021.129966

Niskanen, I., Suopajärvi, T., Liimatainen, H., Fabritius, T., Heikkilä, R., & Thungström, G. (2019). Determining the complex refractive index of cellulose nanocrystals by combination of Beer–Lambert and immersion matching methods. *Journal of Quantitative Spectroscopy and Radiative Transfer, 235*, 1–6. https://doi.org/10.1016/j.jqsrt.2019.06.023

Pakoulev, A., Wang, Z., & Dlott, D. D. (2003). Vibrational relaxation and spectral evolution following ultrafast OH stretch excitation of water. *Chemical Physics Letters, 371*(5–6), 594–600. https://doi.org/10.1016/S0009-2614(03)00314-2

Peltzer, M. A., Salvay, A. G., Delgado, J. F., De La Osa, O., & Wagner, J. R. (2018). Use of residual yeast cell wall for new biobased materials production: Effect of plasticization on film properties. *Food and Bioprocess Technology, 11*, 1995–2007.

Rahmani, R., Beaufort, S., Villarreal-Soto, S. A., Taillandier, P., Bouajila, J., & Debouba, M. (2019). Kombucha fermentation of African mustard (Brassica tournefortii)leaves: Chemical composition and bioactivity. *Food Bioscience, 30* (August 2018), Article 100414. https://doi.org/10.1016/j.fbio.2019.100414

Ramírez Tapias, Y. A., Di Monte, M. V., Peltzer, M. A., & Salvay, A. G. (2022). Bacterial cellulose films production by Kombucha symbiotic community cultured on different herbal infusions. *Food Chemistry, 372*. https://doi.org/10.1016/j.foodchem.2021.131346

Ramírez Tapias, Y. A., Peltzer, M. A., Delgado, J. F., & Salvay, A. G. (2020). Kombucha tea by-product as source of novel materials: Formulation and characterization of films. *Food and Bioprocess Technology, 13*(7), 1166–1180. https://doi.org/10.1007/s11947-020-02471-4

Re, R., Pellegrini, A., Ananth Pannala, M., & Rice-Evans, C. (1999). Antioxidant activity applying an improved abts radical. *Free Radical Biology & Medicine, 26*(98), 1231–1237. https://doi.org/10.1016/S0891-5849(98)00315-3

Roy, S., Gennadios, A., Weller, C. L., & Testin, R. F. (2000). Water vapor transport parameters of a cast wheat gluten film. *Industrial Crops and Products, 11*(1), 43–50. https://doi.org/10.1016/S0926-6690(99)00032-1

Rozenberga, L., Skute, M., Belkova, L., Sable, I., Vikele, L., Semjonovs, P., et al. (2016). Characterisation of films and nanopaper obtained from cellulose synthesised by acetic acid bacteria. *Carbohydrate Polymers, 144*, 33–40. https://doi.org/10.1016/j.carbpol.2016.02.025

Salvay, A. G., Colombo, M. F., & Grigera, J. R. (2003). Hydration effects on the structural properties and haem–haem interaction in haemoglobin. *Physical Chemistry Chemical Physics, 5*(1), 192–197.

Sharma, C., & Bhardwaj, N. K. (2020). Fabrication of natural-origin antibacterial nanocellulose films using bio-extracts for potential use in biomedical industry. *International Journal of Biological Macromolecules, 145*, 914–925. https://doi.org/10.1016/j.ijbiomac.2019.09.182

Silva Júnior, J. C.da, Magnani, M., Almeida da Costa, W. K., Madruga, M. S., Souza Olegário, L., da Silva Campelo Borges, G., et al. (2021). Traditional and flavored kombuchas with pitanga and umbu-cajá pulps: Chemical properties, antioxidants, and bioactive compounds. *Food Bioscience, 44*(September). https://doi.org/10.1016/j.fbio.2021.101380

Szcześniak, L., Rachocki, A., & Tritt-Goc, J. (2008). Glass transition temperature and thermal decomposition of cellulose powder. *Cellulose (London, England), 15*(3), 445–451. https://doi.org/10.1007/s10570-007-9192-2

Vieira, M. G. A., Da Silva, M. A., Dos Santos, L. O., & Beppu, M. M (2011). Natural-based plasticizers and biopolymer films: A review. *European Polymer Journal, 47*(3), 254–263. https://doi.org/10.1016/j.eurpolymj.2010.12.011

Vilela, C., Kurek, M., Hayouka, Z., Röcker, B., Yildirim, S., Dulce, M., et al. (2018). A concise guide to active agents for active food packaging. *Trends in Food Science & Technology, 80*(August), 212–222. https://doi.org/10.1016/j.tifs.2018.08.006

Xia, Z., Singh, A., Kiratitanavit, W., Mosurkal, R., Kumar, J., & Nagarajan, R. (2015). Unraveling the mechanism of thermal and thermo-oxidative degradation of tannic acid. *Thermochimica Acta, 605*, 77–85. https://doi.org/10.1016/J.TCA.2015.02.016

Zhu, F. (2021). Polysaccharide based films and coatings for food packaging: Effect of added polyphenols. *Food Chemistry, 359*(April), Article 129871. https://doi.org/10.1016/j.foodchem.2021.129871